Journal of Bioscience and Bioengineering
VOL. 127 No. 1, 66–72, 2019

www.elsevier.com/locate/jbiosc

Down-regulation of pyruvate decarboxylase gene of white-rot fungus *Phlebia* sp. MG-60 modify the metabolism of sugars and productivity of extracellular peroxidase activity

Taichi Motoda, Megumi Yamaguchi, Taku Tsuyama, and Ichiro Kamei*

Faculty of Agriculture, University of Miyazaki, 1-1 Gakuen-kibanadai-nishi, Miyazaki 889-2192, Japan

Received 4 April 2018; accepted 21 June 2018
Available online 12 July 2018

Ethanologenic white-rot fungus *Phlebia* sp. MG-60-P2 produces ethanol directly from several lignocelluloses. Efficient gene silencing methods are needed for metabolic engineering of this fungus for biorefinery use. In this study, we evaluated the effectiveness of RNAi-mediated silencing of the pyruvate decarboxylase gene of *Phlebia* sp. MG-60-P2 (MG*pdc1*). The RNAi lines generated showed a variety of suppression levels of ethanol production and MG*pdc1* expression, and two selected strains led to different metabolic fluxes, resulting in rapid accumulation of xylitol from xylose. Knockdown lines KD2 and KD10 showed different strength of silencing. The moderate-inhibition line (KD10) showed faster xylitol accumulation from xylose than the severe-inhibition line (KD2). KD2, KD10 and knockout line KO77 showed higher extracellular peroxidase activity than the wild-type. Gene silencing using RNAi for MG*pdc1* in the ethanologenic white-rot fungus *Phlebia* sp. MG-60-P2 is an effective first step in metabolic engineering to produce other chemicals besides ethanol. This high efficiency of transformation and silencing effect will make it possible to cotransform with multiple expression vectors which enhance the minor metabolic pathway or introduce exogenous metabolic reaction in *Phlebia* sp. MG-60-P2.

[**Key words:** Basidiomycete; White-rot fungi; Fermentation; RNAi; Pyruvate decarboxylase; Extracellular peroxidase]

Lignin-degrading basidiomycetes, white-rot fungi, can degrade all the main components of plant cell walls, including cellulose, hemicellulose, and lignin. Recently, it was reported that the marine white-rot fungus *Phlebia* sp. MG-60 could directly produce ethanol from cellulose via saccharification by self-producing cellulase (1). This process, referred to as consolidated bioprocessing, has the potential to decrease the cost of enzymatic saccharification processes (2). *Phlebia* sp. MG-60 also has high selectivity for lignin degradation. Thus, a novel process (integrated fungal fermentation), which unifies aerobic delignification and anaerobic saccharification and fermentation of wood, was proposed for *Phlebia* sp. MG-60 (3). This fungus can selectively degrade lignin in aerobic solid-state fermentation conditions and produce ethanol directly from delignified oak wood in semi-aerobic liquid culture conditions. Additionally, the fungus can ferment glucose, cellulose and xylose (1,4). In culture with xylose, low-level accumulation of xylitol was observed. Filamentous fungi and some yeasts use an oxidoreductive pathway which involves two reactions to catabolize xylose. First, xylose is reduced to xylitol by an NAD(P)H-dependent xylose reductase (XR). Then, xylitol is oxidized to xylulose by an NAD^+-dependent xylitol dehydrogenase (XDR). Xylulose is phosphorylated to xylulose-5-phosphate then further metabolized through the pentose phosphate pathway (5). Therefore, the production of xylitol by *Phlebia* sp. MG-60 suggests that the oxidoreductive pathway is followed by the production of ethanol in *Phlebia* sp. MG-60.

In *Saccharomyces cerevisiae*, pyruvate decarboxylase (PDC) genes directly contribute to ethanol production (6,7). To produce valuable fermentation products such as xylitol, lactic acid, or pyruvate, disruption of PDC is an effective metabolic approach to inhibit ethanol production (8–10). Techniques are available to deplete the activity of specific genes, such as homologous recombination or RNA interference (RNAi). Recently we constructed a MG*pdc1* gene knockout strain of *Phlebia* sp. MG-60 by homologous recombination; however, the efficiency of homologous recombination is <1% in *Phlebia* sp. MG-60 (11). Therefore, more efficient gene silencing methods are needed.

The purpose of this study was to evaluate the effectiveness of MG*pdc1* RNAi-mediated gene silencing in *Phlebia* sp. MG-60. Comparison was made between the consumption of glucose and the production of ethanol as the effect of RNAi-mediated silencing. Then, the accumulation of xylitol from xylose by MG*pdc1*-gene silenced transformants was monitored as the initial step of metabolic engineering of *Phlebia* sp. MG-60. Additionally, the effect of the change of carbon flux on the extracellular peroxidase activity is discussed.

* Corresponding author. Tel./fax: +81 985 58 7181.
E-mail addresses: gb13048@student.miyazaki-u.ac.jp (T. Motoda), meg3-y@cc.miyazaki-u.ac.jp (M. Yamaguchi), tsuyama@cc.miyazaki-u.ac.jp (T. Tsuyama), kamei@cc.miyazaki-u.ac.jp (I. Kamei).

1389-1723/$ – see front matter
https://doi.org/10.1016/j.jbiosc.2018.06.017

MATERIALS AND METHODS

Fungal strain and cultures *Phlebia* sp. strain MG-60 TUFC40001 (Fungus/Mushroom Resource and Research Center, Tottori, Japan) was maintained on potato dextrose agar plates. *Phlebia* sp. strain MG-60-P2 was isolated from the protoplast derived from strain MG-60 to unify the phenotypes of protoplast regenerated strains (11).

Isolation of nucleic acids and cDNA preparation The mycelia from 10-mL liquid cultures were filtered through Miracloth (Calbiochem, San Diego, CA, USA), semi-dried with sterile paper towel, frozen rapidly in liquid nitrogen, and stored at −80°C. The frozen mycelium was ground into powder by crushing with a hammer. DNA was isolated from the mycelium powder with Isoplant (Nippon Gene Co., Ltd., Toyama, Japan). The total RNA was prepared using a combination of Plant RNA Isolation Reagent (Invitrogen Corp., Carlsbad, CA, USA) and TRIzol reagent (Invitrogen Corp.). The RNA obtained was washed with 75% ethanol and dissolved in RNase-free water. The amount and quality of RNA were calculated from the absorbances at 260 and 280 nm cDNA was synthesized in a 20-μL reaction mixture that included 1 μg of total RNA, 1 μM oligo (dT)-adapter primer containing an M13 primer M4 sequence, 10 U of RNase inhibitor, and 10 U of AMV Reverse Transcriptase (Takara Bio Inc., Kusatsu, Japan), used according to the manufacturer's instructions. The reaction was carried out for 60 min at 45°C, then the samples were heated for 5 min at 95°C to terminate the reaction. Finally, the reaction mixture was diluted 1:100 with RNase-free water and a 1-μL sample was used for RT-PCR analysis to amplify the pyruvate decarboxylase gene (*pdc*) partial sequence from *Phlebia* sp. MG-60 by using specific primers listed in Table S1.

Preparation of knockdown construct The full-length MG*pdc1* gene was isolated in our previous study (11). A 4916-bp MG*pdc1* genomic fragment containing 1531 bp of promoter region, 2166 bp of coding region, and 1219 bp of terminator region was cloned (accession no. LC214886) (Fig. 1). From the cDNA sequence, the MGpdc1 protein was encoded by 1818 bp (605 amino acids). A knockdown construct for MG*pdc1* was prepared as follows (Fig. 1). Polymerase chain reaction (PCR) was performed to amplify fragments of MG*pdc1* and *β*-glucuronidase (GUS), using the primer pairs *mgPDC-F1i*/*mgPDC-R1i*, *mgPDC-F2i*/*mgPDC-R2i*, and *GUS-F*/*GUS-R* (Table S1). All these fragments were ligated into the *Bam*HI site in vector pUC19 using the In-Fusion cloning system (Takara Bio) to produce the plasmid shown in Fig. 1B. The cloned construct was amplified using the primer set *mgPDC-Asc1* to add an *Asc*I restriction site (sequence 1). DNA including the Pb*gpd* promoter, Pb*gpd* terminator and *Asc*I restriction site was amplified using the primer set *PbGPD-Asc-F1*/*PbGPD-Asc-R1* from the vector pMD20 which includes the Pb*gpd* genomic sequence (12) (sequence 2). pMGPDC-RNAi was constructed by ligation of sequence 1 and sequence 2 (Fig. 1). KOD FX Neo (Toyobo, Osaka, Japan) was used for all PCR amplifications. The PCR products were subcloned into vector pUD19 (Takara Bio), and the resulting ligation products were transformed into *Escherichia coli* strain JM109 according to the manufacturer's protocol (Takara Bio). Clones were sequenced by a dideoxy method (BigDye Terminator v3.1 Cycle Sequencing Kit, Thermo Fisher Scientific Inc., Waltham, MA, USA) with a sequencer (model 3500xL; Applied Biosystems, Foster City, CA, USA).

Incubation for transcriptional analysis Mycelium was preincubated in 100-mL Erlenmeyer flasks containing 18 mL of basal liquid medium (10 g/L yeast extract, 10 g/L KH_2PO_4, 2 g/L $(NH_4)_2SO_4$, 0.5 g/L $MgSO_4{\cdot}7H_2O$) (pH 6.0) (13) without glucose for 5 d. Then, 2 mL of 20% (w/v) glucose solution was added through a 0.22-μm filter, followed by further incubation at 28°C for 72 h. After incubation, the whole culture was separated into a mycelium and extracellular fluid by centrifugation. Then, total RNA was extracted from the mycelium and ethanol production was measured by HPLC as described below. Real-time fluorescence-based reverse transcription PCR (real-time PCR) was performed in a final volume of 10 μL with an iCycler (Bio-Rad Laboratories Inc., Hercules, CA, USA). cDNA was synthesized in a final volume of 20 μL that included 1 μg of total RNA, 1 μM oligo(dT)18 primer, 10 U of RNase inhibitor, and 10 U of AMV Reverse Transcriptase, according to the manufacturer's instructions. After reverse transcription for 60 min at 45°C, the samples were heated for 5 min at 95°C to terminate the reaction. The SYBR Premix Ex *Taq* kit (Takara Bio) was used for real-time PCR according to the manufacturer's instructions with a final concentration of 0.2 μM for each gene specific primer (*MG-PDC-real-1F* and *MG-PDC-real-1R*). PCR amplification was performed as follows: an initial denaturation at 95°C for 30 s, then 40 cycles of denaturation at 95°C for 5 s and annealing at 58°C for 30 s. Amplicon specificity was verified by melting-curve analysis conducted at 55−95°C with stepwise fluorescence acquisition. *Gpd* (GenBank accession number: AB360638) was used as the reference gene (14); the ratio of gene specific expression was defined as expression relative to *gpd* gene expression. The quantification of each gene was calculated by the standard curve constructed with C_t value.

Transformation Protoplast isolation and polyethylene glycol (PEG)-mediated cotransformation assays with MG-60-P2 were performed following our previous report (12). Insertion of the construct was confirmed by PCR using primers *GUS-F*/*GUS-R*. The resulting 144 hygromycin-resistant strains were used as PCR templates to determine p*MGPDC-RNAi* insertion. Finally, 108 strains were identified as cotransformants of p*MGPDC-RNAi* and p*PbGPD-HPT*. The resulting efficiency of cotransformation was 75% (108 cotransformants/144 hygromycin-resistant strains). Ethanol fermentation ability from glucose was evaluated for isolated transformants, as described below.

Fermentation Ethanol fermentation ability was evaluated for the isolated transformants as described previously (1) with slight modification. Briefly, 20 mL of basal liquid medium containing 2% glucose, xylose or 0.4 g of unbleached hardwood kraft pulp (UHKP) in a 100 mL Erlenmeyer flask was autoclaved. UHKP was kindly gifted from Oji Paper Co., Ltd., Tokyo, Japan. Six mm diameter discs were punched from the edge of the mycelium incubated on potato dextrose agar plates. A disk was placed into a 100 mL Erlenmeyer flask containing 20 mL of basal liquid medium with the carbon sources mentioned above. After sealing with a silicon plug stopper (semi-aerobic conditions), the culture was incubated statically at 28°C. The resulting supernatant was analyzed by high performance liquid chromatography (HPLC) to quantify the amount of ethanol and monosaccharides. To examine the time course of conversion of xylose, 30 mL of basal medium containing 2% xylose in a 50 mL Erlenmeyer flask was autoclaved. After placing a disk of mycelium and sealing with a silico plug stopper (aerobic conditions), the

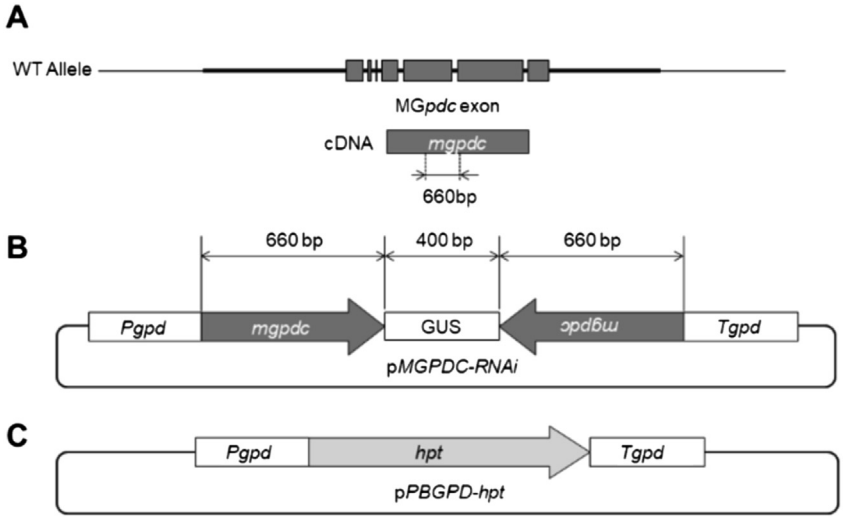

FIG. 1. MG*pdc1* knockdown and selection vectors. (A) Schematic representation of the MG*pdc1* gene. Shaded boxes indicate MG*pdc1* exons. (B) Schematic representation of the MG*pdc1* knockdown vector p*MGPDC-RNAi*. *Pgpd* and *Tgpd* are respectively the promoter and terminator of the glyceraldehyde-3-phosphate dehydrogenase (*gpd*) gene of *Phlebia brevispora*. *mgpdc*, part of the MG*pdc1* gene, is indicated as shaded boxes. GUS is part of the *β*-glucuronidase sequence. (C) Schematic representation of the selection vector p*PBGPD-hpt*. Hpt, hygromycin B resistance gene.

culture was incubated on a rotary shaker at 120 rpm in the dark at 28°C. One milliliter of the medium was collected every 24 h and quantified the amount of ethanol, xylitol, and remaining xylose by HPLC.

Enzyme assay Wild-type strain P2, knockdown strains KD2 (the severe-inhibition of expression of MG*pdc1* line) and KD10 (the moderate-inhibition of expression of MG*pdc1* line), and knockout strain KO77 (11) were cultured in 10 mL Kirk's low-nitrogen medium (Kirk LN) (15) at pH 4.5 in 100-mL Erlenmeyer flasks. Crude enzymes were prepared by filtration and centrifugation (15,000 × *g*, 4°C, 10 min). Separated mycelia were dried in an oven at 105°C overnight to determine the weight of mycelium. Total phenol oxidase (TPO) activity was determined spectrophotometrically by measuring the oxidation of 2,6-dimethoxyphenol to coerulignone (ε = 49.6 $mM^{-1}cm^{-1}$) in 50 mM malonate buffer (pH 4.5) containing 1.0 mM $MnSO_4$ 1.0 mM 2,6-dimethoxyphenol and 0.2 mM H_2O_2 at 469 nm. Laccase activity was determined spectrophotometrically by measuring the oxidation of 2,6-dimethoxyphenol in 50 mM malonate buffer (pH 4.5) containing 1.0 mM 2,6-dimethoxyphenol at 469 nm. Peroxidase activity was calculated by the following formula.

$$(\text{Peroxidase activity}) = (\text{TPO activity}) - (\text{Laccase activity}) \quad (1)$$

One unit of peroxidase activity was defined as the amount of enzyme required to oxidize 1 μmol of 2,6-dimethoxyphenol per min. The remaining glucose and the ethanol yield was monitored by HPLC analysis, as described below.

Analytical methods After the appropriate incubation periods, the mycelium was removed from culture by centrifugation at 13,000 × *g* for 10 min. The resulting supernatant was analyzed by high-performance liquid chromatography (HPLC) to quantify the amount of ethanol, monosaccharides and disaccharides after filtration with a membrane filter (0.45-μm). HPLC system was composed by a RID-10A differential refractive index detector (Shimadzu Corp., Kyoto, Japan) with an IC Sep COREGEL-87H3 column (7.8 × 300 mm; Chrom Tech, Inc., Apple Valley, MN, USA). The supernatant was eluted with 5 mM sulfuric acid solution at a flow rate of 0.6 mL/min.

Mycelial growth The fungus was grown on PDA in petri dishes at 28°C. Mycelial disks (6-mm diameter) were taken from the margins of 4-day-old fungal colonies and placed on new PDA plates. The radius of the fungal colony was measured every day.

RESULTS AND DISCUSSION

Effect of knockdown of MG*pdc1* on glucose fermentation Glucose fermentation by the 108 isolated transformants was tested. The usage trends of glucose and production of ethanol by the transformants and wild-type *Phlebia* sp. MG-60-P2 are shown in Fig. 2. Ethanol productivities of all the transformants were lower than that of *Phlebia* sp. MG-60-P2. The amounts of glucose use and ethanol production were well correlated. From these strains, knockdown strain No. 2 (KD2) and knockdown strain No. 10 (KD10) were selected for further studies because of their distinct ethanol productivities. Fig. 3 shows the time course of the

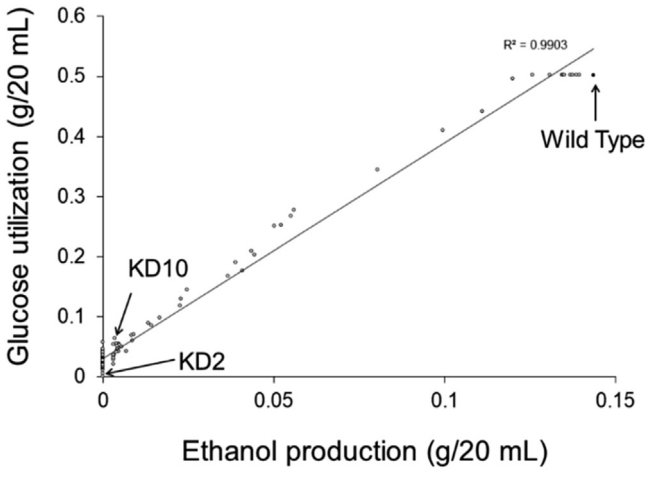

FIG. 2. Effects of RNAi transfection for *Phlebia* sp. MG-60 P2. The correlation between glucose use and ethanol production by transformants is shown. Knockdown strain No. 2 (KD2) and knockdown strain No. 10 (KD10) were selected for further studies.

ethanol yields and the transcriptional levels of MG*pdc1* in fermentation by the wild-type, KD2 and KD10. The productivity of ethanol by KD2 was strongly inhibited, and KD10 produced ethanol with a delay (Fig. 3A). The transcription level of MG*pdc1* was decreased in both KD2 and KD10 compared to the wild-type (Fig. 3B). The transcription level of MG*pdc1* in KD2 was very low, and below that in KD10, which is in consistent with the ethanol productivity of each strain. In other words, the expression of MG*pdc1* was highly suppressed in KD2, and the suppression of MG*pdc1* in KD10 was lower than that of KD2. The stability of the quantitative trends for the silencing of ethanol fermentation was proved by several tests (data not shown). It was concluded that MG*pdc1* gene silencing by RNAi could be achieved efficiently, and that knockdown strains with variation were constructed for further experiments.

Fermentation of xylose *Phlebia* sp. MG-60 can ferment xylose into ethanol and xylitol (3). To evaluate the effect of knockdown of MG*pdc1*, xylose was used as substrate. Fig. 4 shows the time course of xylose use and the production of ethanol and xylitol. Xylose was consumed rapidly by strain MG-60-P2, then ethanol and a little xylitol accumulated (Fig. 4A). In contrast, there was little consumption of xylose and no production of ethanol by strain KD2 (Fig. 4B). Rapid accumulation of a low amount of xylitol was observed in the initial 4 d of incubation of strain MG-60-P2, and the level of xylitol was slightly decreased after 4 d (Fig. 4A). For strain KD2, the consumption of xylose was slow; however, xylitol accumulated incrementally in the late stages of incubation. This trend of slow consumption of xylose and accumulation of xylitol was identical to the results for knockout strain KO77 in our previous report (11). Normally, xylitol is produced by the reduction of xylose by NAD(P)H-dependent XR. Xylitol is then oxidized to xylulose by NAD^+-dependent XDR (5). We have discussed previously that the accumulation of xylitol in knockout line KO77 might be caused by the inactivation of XDR, associated with depletion of NAD^+ induced by the deletion of the MG*pdc1* gene (11). These results may indicate the interlocking of metabolic flux between the oxidoreductive pathway for catabolism of xylose and pyruvate decarboxylation via NADH reoxidation.

Interestingly, transformant KD10 which produces ethanol with a delay showed different results from KD2 and the wild-type strain MG-60-P2. The consumption of xylose by KD10 was slower than that by MG-60-P2, but faster than that by KD2. The accumulation of xylitol by KD10 was faster than that by KD2 (Fig. 4B,C). The concentrations of xylitol produced by KD2 and KD10 after 5 d of incubation were 0.5 and 1.8 mg/mL, respectively; thus, the xylitol concentration in the culture of KD10 was 3.6-times higher than that for KD2 (Fig. 4B,C). The highest concentration of xylitol (4.1 mg/mL) was observed after 9 d of incubation of KD10 (Fig. 4C). These results, and the correlation between the amount of glucose use and ethanol production (Fig. 2), suggest that strong silencing of the MG*pdc1* gene causes a severe decrease of carbon flux into glycolysis for pyruvate production from carbohydrate, and that partial suppression but not knockout of MG*pdc1* improves the accumulation of xylitol.

Fermentation of UHKP *Phlebia* sp. MG-60 can ferment cellulose materials into ethanol (1,3). To evaluate the effect of knockdown of MG*pdc1* on saccharification and fermentation of cellulose, UHKP was used as substrate. Fig. 5 shows the production of ethanol and glucose from UHKP by MG-60-P2 (the wild-type strain) (Fig. 5A), and strains KD2 (Fig. 5B) and KD10 (Fig. 5C). At 5 d incubation, KD10 produced less ethanol than the wild-type, which is consistent with the result that the fermentation activity for monomeric sugar of KD10 was drastically lower than that of the wild-type (Figs. 2 and 3). After

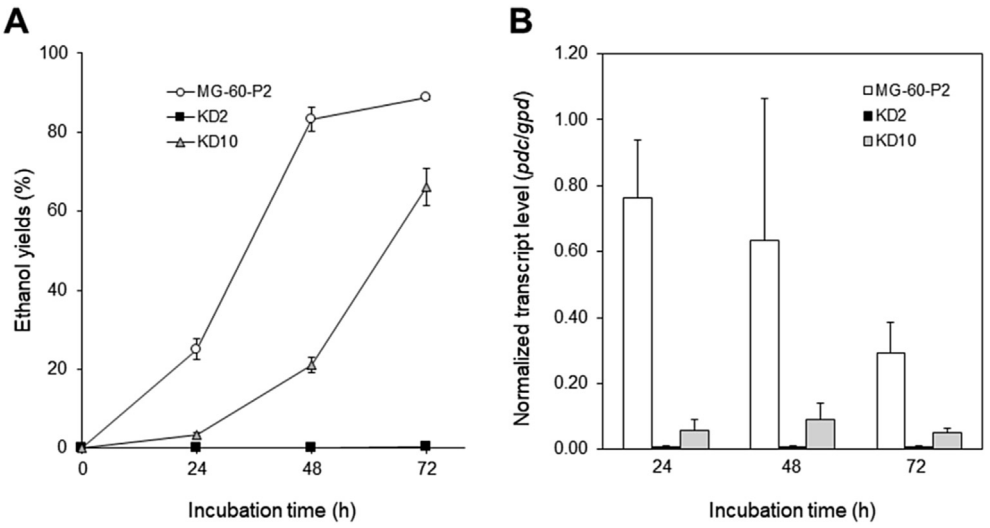

FIG. 3. Suppression of ethanol production and MG*pdc1* transcription in strains KD2 and KD10. (A) Suppression of ethanol production in KD2 and KD10. Open circles, closed squares, and shaded triangles indicate wild-type MG-60-P2, KD2, and, KD10 respectively. (B) Suppression of MG*pdc1* transcription in KD2 and KD10 confirmed by real-time PCR. Open bars, closed bars, and shaded bars indicate wild-type MG-60-P2, KD2, and KD10, respectively. The transcription level of the MG*pdc1* gene was normalized by the transcription level of the constitutively-expressed *gpd* gene. Data for wild-type MG-60-P2 were collected at the time of a previous study (11). Data are means ± SD of three individual experiments.

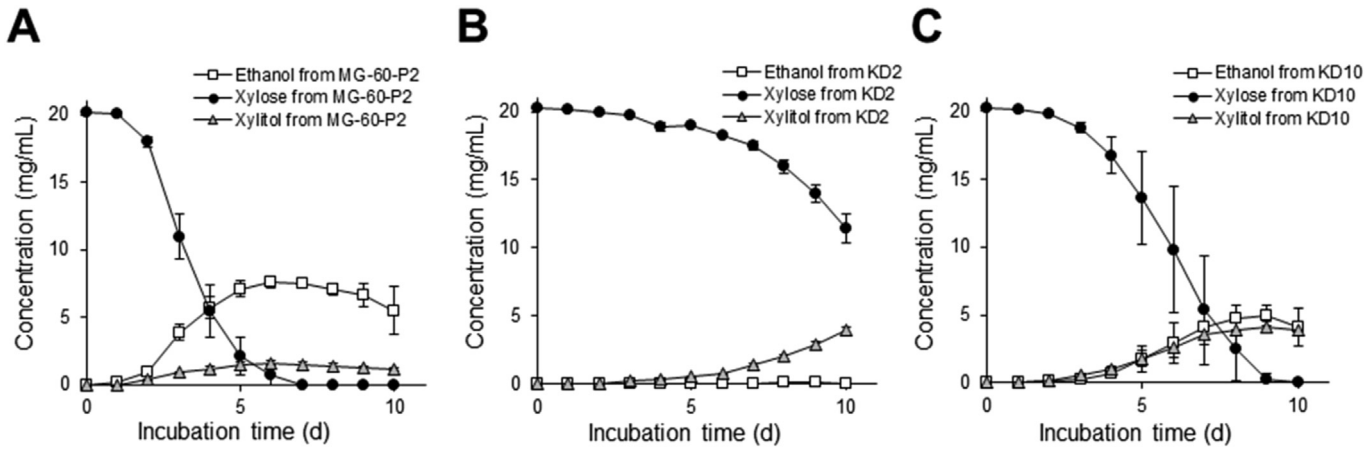

FIG. 4. Fermentation of xylose by *Phlebia* sp. MG-60-P2, KD2 and KD10. Time courses of fermentation of xylose by wild-type MG-60-P2 (A), KD2 (B) and KD10 (C). Open squares, closed circles, and shaded triangles indicate ethanol, xylose, and xylitol, respectively. Data for wild-type MG-60-P2 (A) were collected at the time of a previous study (11). Data are means ± SD of three individual experiments.

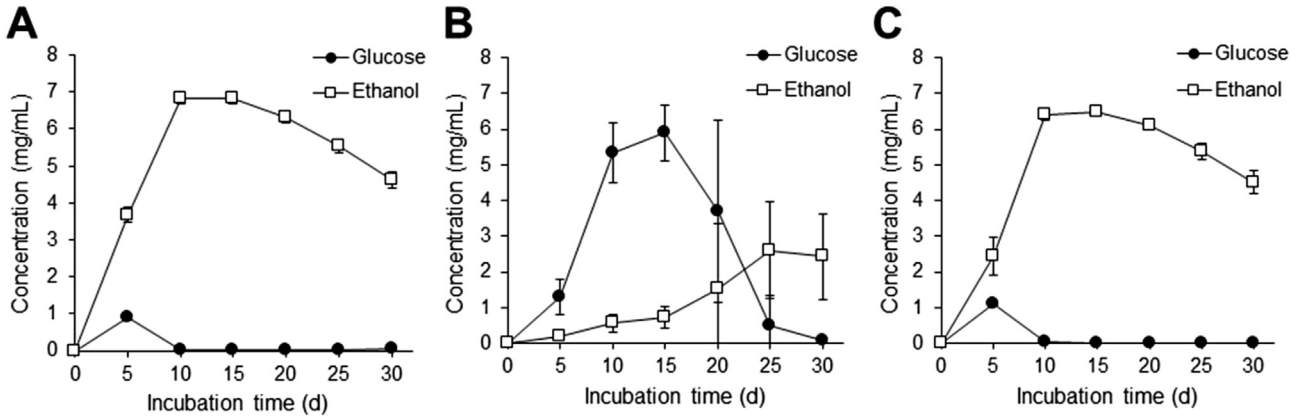

FIG. 5. Fermentation of unbleached hardwood kraft pulp (UHKP) by strains KD2 or KD10. Time courses of glucose and ethanol production from UHKP by wild-type MG-60-P2 (A), KD2 (B) and KD10 (C). Closed circles and open squares indicate glucose and ethanol, respectively. Data for wild-type MG-60-P2 (A) were collected at the time of a previous study (11). Data are means ± SD of three individual experiments.

10 d of incubation, KD10 produced ethanol from cellulose and there was no accumulation of glucose, which was identical to strain MG-60-P2. Moderate downregulation of the MG*pdc1* gene appears not to affect cellulose degradation and glucose consumption in long-term incubation.

In contrast, accumulation of glucose and delayed production of ethanol was observed in culture of KD2 (Fig. 5B) in which MG*pdc1* expression was downregulated severely (Fig. 3). This delay of ethanol production with late glucose consumption was caused by severe knockdown, but not knockout, of the MG*pdc1* gene; the MG*pdc1* knockout line (KO77) showed glucose accumulation with little ethanol production even after 20 d of incubation (11). These results suggest that downregulation by RNAi may produce knockdown lines with varied amounts of metabolite flux and accumulation, which could be suitable for further metabolic engineering or application for metabolite production.

Enhancement of extracellular phenol oxidase activity MG*pdc*-knockout line KO77 was generated in our previous study (11). To examine the effect of the change of carbon flux from ethanol fermentation into the TCA cycle, the peroxidase activity was monitored in low-nitrogen medium. Interestingly, higher peroxidase activity was observed in all MG*pdc* knockdown or knockout strains than in the wild-type strain MG-60-P2 (Fig. 6). Up-regulation and activation of extracellular peroxidase and TCA cycle was reported by the addition of aromatic compound in the culture with white rot fungus *Phanerochaete chrysosporium* (16). Therefore, TCA cycle seem to be one of the factors for the production of extracellular peroxidase. In low-nitrogen medium, wild-type strain MG-60-P2 produced ethanol preferentially, but the transformants showed low or no ethanol production (Fig. 7A). Consumption of glucose in wild-type culture was rapid, and it was used completely by 10 d of incubation. Glucose consumption in the cultures with all MG*pdc* knockdown or knockout strains was slow and glucose remained even after 14 d (Fig. 7B). Remarkable initial growth of the mycelium of wild-type MG-60-P2 was observed in this culture, whereas the growth of transformants was slower (Fig. 7C). These results suggest that ethanol fermentation was used preferentially for the fast growth of mycelium in liquid culture, and that carbon flux into the TCA cycle was very limited.

It is assumed that the down regulation of ethanol fermentation pathway may lead to increase of carbon flow into TCA cycle in low-nitrogen medium. The phenomenon of peroxidase activity enhancement by the down regulation of MG*pdc1* might be caused by promoting heme synthesis depends on the change of carbon flux from ethanol fermentation into the TCA cycle. Many white-rot fungi produce multiple extracellular ligninolytic enzymes (17). It was reported that *Phlebia* sp. MG-60 produced manganese peroxidases (MnP) (13). Heme, which is essential for peroxidases, is produced by the combination of porphyrin with iron. Two alternative routes have been reported for the formation of aminolevulinic acid (ALA) which is an intermediate in porphyrin synthesis. Succinyl-CoA and glycine are condensed to produce ALA by ALA synthase in animals and fungi (18,19). In the white-rot fungus *P. chrysosporium*, the

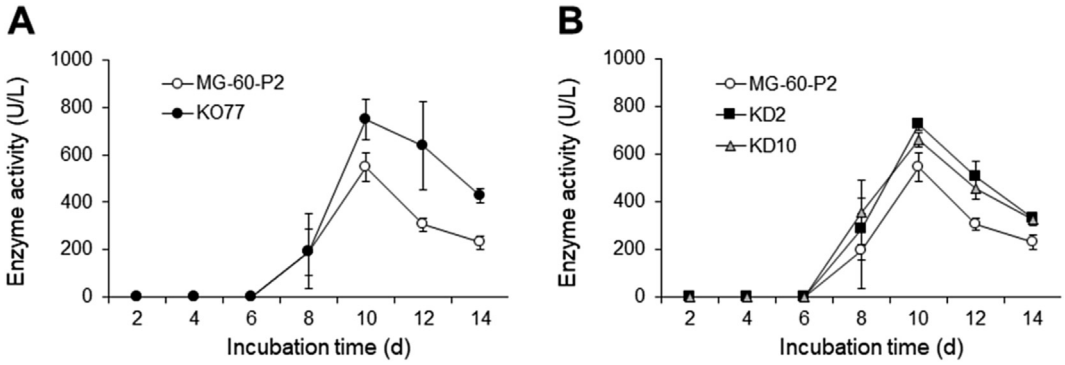

FIG. 6. The effect of suppression of ethanol fermentation on peroxidase activity in low-nitrogen medium. Time course of extracellular peroxidase activity in cultures of knockout line KO77 (A) and knockdown lines KD2 and KD10 (B), compared with wild-type MG-60-P2.

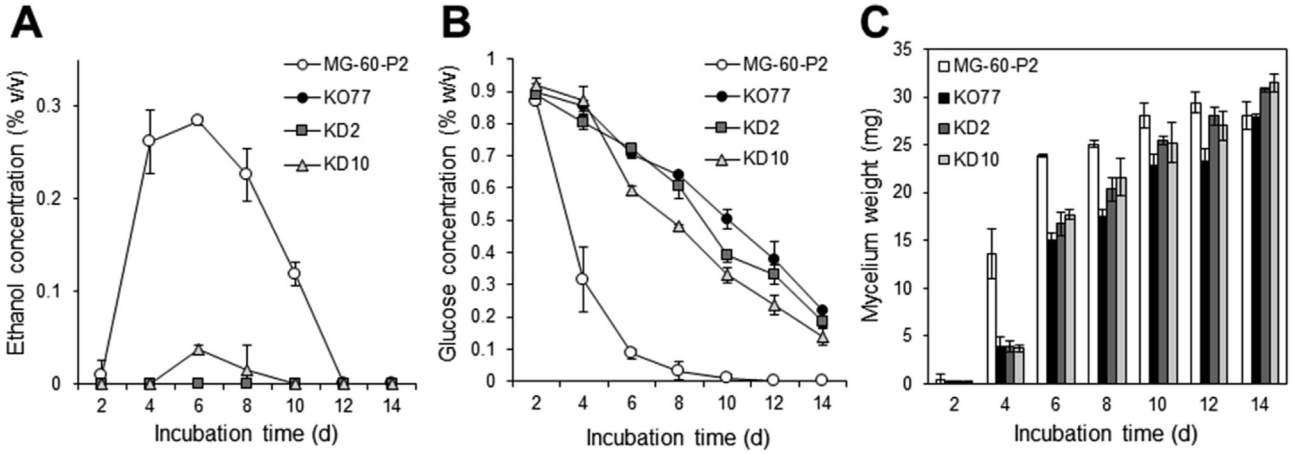

FIG. 7. The effect of suppression of the MG*pdc1* gene on the production of ethanol (A), glucose consumption (B), and mycelial growth (C), in low-nitrogen medium. Data are means ± SD of three individual experiments.

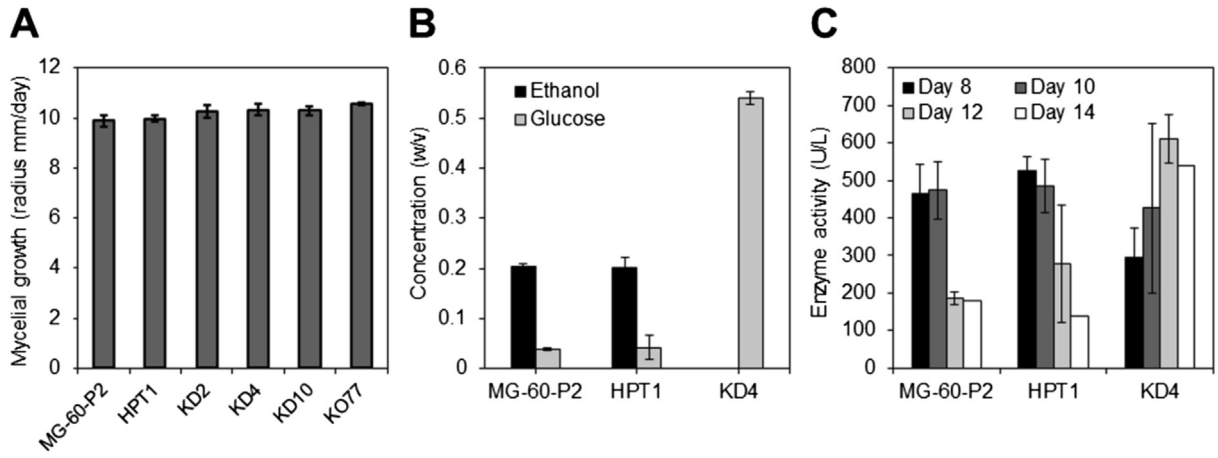

FIG. 8. The mycelial growth on PDA medium (A), fermentation traits of MG-60-P2, HPT1, and KD4 in low-nitrogen medium (B), and extracellular peroxidase activity in low-nitrogen medium of MG-60-P2, HPT1, and KD4 (C). HPT1, which has p*PbGPD-HPT* only; KD4, which has p*MGPDC-RNAi* and exhibits similar phenotypes to KD2. Data are means ± SD of three individual experiments. The values of enzyme activity (C: day 14) show the average of duplicated sample.

exogenous addition of vanillin, an intermediate of lignin biodegradation, upregulated the expression of the ALA synthase gene and the production of MnP (16). Expression of the gene encoding ALA synthase corresponded temporally with the expression and activity of MnP in *Phanerochaete sordida* (20). These results suggested that TCA cycle metabolic flux into heme biosynthesis is linked with the production of MnP. In the present study, suppression of ethanol production by downregulating the MG*pdc1* gene seems to enhance peroxidase production, which may result from the change of carbon flux into the TCA cycle and constant ALA synthesis because of constant glucose uptake (Fig. 7B). There are many reports about the productivity of peroxidase in liquid culture by white-rot fungi, however, so far as we know, there is no discussion of carbon flux competition with ethanol fermentation. In our previous study, many white-rot fungi could ferment ethanol from glucose in liquid culture (1,3). We therefore propose that inhibition of ethanol fermentation is one of the ways to enhance the production of lignolytic enzymes in liquid culture.

Supporting experiments by other transformants To confirm that the enhancement of extracellular peroxidase activity was caused by gene silencing of MG*pdc1*, additional transformants HPT1 which has p*PbGPD-HPT* only and KD4 which exhibits similar phenotypes to KD2 by gene silencing of MG*pdc1* were used for additional experiments. There were no significant difference of mycelial growth between each transformant and wild-type strain MG-60-P2 in PDA medium (Fig. 8A). This result indicated that the transfection of p*MGPDC-RNAi* or p*PbGPD-HPT* did not induce any cytotoxicity. Therefore, it was supported that the inhibition of glucose consumption and initial growth of MG*pdc1* down-regulated strains in liquid culture (Fig. 7) were caused by inhibition of ethanol fermentation. There was no inhibition of ethanol fermentation or glucose consumption in liquid culture with HPT1 showing similar phenotype to wild-type strain MG-60-P2 (Fig. 8B). Glucose consumption and ethanol production were inhibited severely in the culture with KD4. The tendency of KD4 to accumulate xylitol from xylose and glucose from cellulose is similar to that of KD2 (data not shown). Peroxidase production in the culture with HPT1 showed similar pattern to that in the culture with wild-type strain MG-60-P2. However, the production of extracellular peroxidase activity in the culture with KD4 tended to increase ($P < 0.05$ at day 12) compared with HPT1 and MG-60-P2. These results supported our conclusion that inhibition of ethanol fermentation by down-regulation of MG*pdc1* enhanced the production of extracellular peroxidase activity.

Conclusion Gene silencing of MG*pdc1* using RNAi in the ethanologenic white-rot fungus *Phlebia* sp. MG-60-P2 is an effective first step in metabolic engineering by inhibiting ethanol production. The RNAi generated lines showed a variety of suppression levels of MG*pdc1* and this variation changed the metabolic flux, resulting in rapid accumulation of xylitol from xylose. Furthermore, suppression of MG*pdc1* enhanced the productivity of extracellular peroxidase in liquid culture. These results demonstrate that RNAi method and silencing of MG*pdc1* are good tools to generate engineered white-rot fungi for biorefinery use of lignocellulosic biomass.

Supplementary data related to this article can be found at https://doi.org/10.1016/j.jbiosc.2018.06.017.

ACKNOWLEDGMENTS

This work was supported partially by the Science and Technology Research Promotion Program for Agriculture, Forestry, Fisheries and Food Industry (27006A) from the Ministry of Agriculture, Forestry, and Fisheries of Japan. This work was supported in part by a Grant-in-Aid for Scientific Research from the Ministry of Education, Culture, Sports, Science and Technology of Japan (grant no. 18H02257 and 17K19296).

References

1. **Kamei, I., Hirota, Y., Mori, T., Hirai, H., Meguro, S., and Kondo, R.:** Direct ethanol production from cellulosic materials by the hypersaline-tolerant white-rot fungus *Phlebia* sp. MG-60, Bioresour. Technol., **112**, 137–142 (2012).
2. **Lynd, L. R., Van Zyl, W. H., McBride, J. E., and Laser, M.:** Consolidated bioprocessing of cellulosic biomass: an update, Curr. Opin. Biotechnol., **16**, 577–583 (2005).
3. **Kamei, I., Hirota, Y., and Meguro, S.:** Integrated delignification and simultaneous saccharification and fermentation of hard wood by a white-rot fungus, *Phlebia* sp. MG-60, BioResources, **9**, 5114–5124 (2014).
4. **Kamei, I., Hirota, Y., and Meguro, S.:** Direct fungal production of ethanol from high-solids pulps by the ethanol-fermenting white-rot fungus *Phlebia* sp. MG-60, BioResources, **9**, 5114–5124 (2014).
5. **Jeffries, T. W.:** Engineering yeasts for xylose metabolism, Curr. Opin. Biotechnol., **17**, 320–326 (2006).
6. **Schmitt, H. D., Ciriacy, M., and Zimmermann, F. K.:** The synthesis of yeast pyruvate decarboxylase is regulated by large variations in the messenger RNA level, Mol. Gen. Genet., **192**, 247–252 (1983).
7. **Hohmann, S.:** Characterization of PDC6, a third structural gene for pyruvate decarboxylase in *Saccharomyces cerevisiae*, J. Bacteriol., **173**, 7963–7969 (1991).
8. **Ishida, N., Saitoh, S., Onishi, T., Tokuhiro, K., Nagamori, E., Kitamoto, K., and Takahashi, H.:** The effect of pyruvate decarboxylase gene knockout in *Saccharomyces cerevisiae* on L-lactic acid production, Biosci. Biotechnol. Biochem., **70**, 1148–1153 (2006).

9. **Stovicek, V., Borodina, I., and Forster, J.:** CRISPR-Cas system enables fast and simple genome editing of industrial *Saccharomyces cerevisiae* strains, Metab. Eng. Commun., **2**, 13–22 (2015).
10. **Song, J.-Y., Park, J.-S., Kang, C. D., Cho, H.-Y., Yang, D., Lee, S., and Cho, K. M.:** Introduction of a bacterial acetyl-CoA synthesis pathway improves lactic acid production in *Saccharomyces cerevisiae*, Metab. Eng., **35**, 38–45 (2016).
11. **Tsuyama, T., Yamaguchi, M., and Kamei, I.:** Accumulation of sugar from pulp and xylitol from xylose by pyruvate decarboxylase-negative white-rot fungus *Phlebia* sp. MG-60, Bioresour. Technol., **238**, 241–247 (2017).
12. **Yamasaki, Y., Yamaguchi, M., Yamagishi, K., Hirai, H., Kondo, R., Kamei, I., and Meguro, S.:** Expression of a manganese peroxidase isozyme 2 transgene in the ethanologenic white rot fungus *Phlebia* sp. strain MG-60, SpringerPlus, **3**, 699 (2014).
13. **Okamoto, K., Imashiro, K., Akizawa, Y., Onimura, A., Yoneda, M., Nitta, Y., Maekawa, N., and Yanase, H.:** Production of ethanol by the white-rot basidiomycetes *Peniophora cinerea* and *Trametes suaveolens*, Biotechnol. Lett., **32**, 909–913 (2010).
14. **Kamei, I., Daikoku, C., Tsutsumi, Y., and Kondo, R.:** Saline-dependent regulation of manganese peroxidase genes in the hypersaline-tolerant white rot fungus *Phlebia* sp. strain MG-60, Appl. Environ. Microbiol., **74**, 2709–2716 (2008).
15. **Tien, M. and Kirk, T. K.:** Lignin peroxidase of *Phanerochaete chrysosporium*, Methods Enzymol., **161B**, 238–249 (1988).
16. **Shimizu, M., Yuda, N., Nakamura, T., Tanaka, H., and Wariishi, H.:** Metabolic regulation at the tricarboxylic acid and glyoxylate cycles of the lignin-degrading basidiomycete *Phanerochaete chrysosporium* against exogenous addition of vanillin, Proteomics, **5**, 3919–3931 (2005).
17. **Lundell, T. K., Makela, M. R., and Hilden, K.:** Lignin-modifying enzymes in filamentous basidiomycetes – ecological, functional and phylogenetic review, J. Basic Microbiol., **50**, 5–20 (2010).
18. **Fukuda, H., Casas, A., and Batlle, A.:** Aminolevulinic acid: from its unique biological function to its star role in photodynamic therapy, Int. J. Biochem. Cell Biol., **37**, 272–276 (2005).
19. **Heinemann, I. U., Jahn, M., and Jahn, D.:** The biochemistry of heme biosynthesis, Arch. Biochem. Biophys., **474**, 238–251 (2008).
20. **Misumi, K., Sugiura, T., Yamaguchi, S., Mori, T., Kamei, I., Hirai, H., Kawagishi, H., and Kondo, R.:** Cloning and transcriptional analysis of the gene encoding 5-aminolevulinic acid synthase of the white-rot fungus *Phanerochaete sordida* YK-624, Biosci. Biotechnol. Biochem., **75**, 178–180 (2011).